



Original Paper

# Advantageous Seepage Channel in Coal Seam and its Effects on the Distribution of High-yield Areas in the Fanzhuang CBM Block, Southern Qinshui Basin, China

Yaning Wu,<sup>1,2</sup> Shu Tao,<sup>1,2,4,5</sup> Wenguang Tian,<sup>3</sup> Hao Chen,<sup>3</sup> and Shida Chen<sup>1,2</sup>

Received 12 November 2020; accepted 28 February 2021  
Published online: 30 March 2021

Results of stress sensitivity experiments show that, when the confining pressure reaches 15.5 MPa, six coal cores have strong stress sensitivity effect (SSE) and cleat compressibility varying from 0.0286 to 0.0725 MPa<sup>-1</sup>. The development of coalbed methane (CBM) is a process of drainage and pressure reduction, which causes inevitable stress-related damage to coal reservoirs. CBM production is affected by different stress-related damage levels, and the damage level depends on different reservoir conditions, working systems, and development stages. The Gu, Huagu, and Pu-Punan zones have high-yield wells with NW–SE distribution, while the Huayna and Huaxi zones have high-yield wells with NE–SW distribution. Based on the stress damage mechanism of reservoir permeability, the factors that control SSE are tectonic stress field, reservoir pressure, and fracture pressure, which in turn affect the productivity changes of CBM wells.

**KEY WORDS:** Stress sensitivity effect, CBM wells, Gas production, High-yield area, Fanzhuang Block.

## INTRODUCTION

By the end of 2018, 18,850 coalbed methane (CBM) wells had been drilled in major CBM basins in China, of which more than 15,000 were in production. However, the ground CBM production was only 5.41 billion m<sup>3</sup> (bcm) in 2018 (Tao, Chen, et al., 2019). Low annual production is caused mainly by

the low averaging production rate due to various geological and engineering factors (Tao et al., 2014; Tao, Chen, et al., 2019; Ye et al., 2013; Zhao et al., 2015a). Regarding the factors that affect CBM production, permeability is a key geological parameter that cannot be ignored (Men et al., 2021; Zhao et al., 2015a; Chen et al., 2018). The development degree and spatial distribution of cleat system (including butt cleat and face cleat, the angle between the two is ~ 90°) have an important impact on coal permeability (Bell, 2006; Laubach et al., 1998).

During the development of CBM, under the action of effective stress (the dissimilarity between the total stress perpendicular to the fractures' direction and the fluid stress within the holes and fractures), matrix shrinkage, and Klingberg effect, the coal reservoir permeability changes dynamically (Kumar et al., 2012). In the early stage of CBM development, the permeability of coal reservoirs is

<sup>1</sup>School of Energy Resources, China University of Geosciences (Beijing), Beijing 100083, People's Republic of China.

<sup>2</sup>Coal Reservoir Laboratory of National Engineering Research Center of Coalbed Methane Development & Utilization, Beijing 100083, People's Republic of China.

<sup>3</sup>PetroChina Research Institute of Petroleum Exploration and Development, Beijing 100083, People's Republic of China.

<sup>4</sup>Coal Reservoir Laboratory of National CBM Engineering Center, China University of Geosciences, Beijing 100083, People's Republic of China.

<sup>5</sup>To whom correspondence should be addressed; e-mail: peach888@163.com

affected greatly by the effective stress, and the permeability drops rapidly with increase in effective stress (Yan et al., 2019; Zhang et al., 2019). In the stage of co-production of gas and water, effective stress and matrix shrinkage effects control simultaneously the dynamic changes of coal permeability, and the permeability gradually stops decreasing or even rebounds (Mazumder et al., 2012; Seidle & Huit, 1995). In the main gas production stage, with continuous desorption, diffusion, seepage and output of CBM, coal permeability is controlled by the above three effects (Li et al., 2014). Generally, the stress sensitivity effect (SSE) of permeability acts on the entire drainage stage of CBM wells and is the main factor affecting the permeability of coal reservoirs.

Scholars have applied various methods to research the relationship between coal permeability and stress. These studies have concluded that, as the effective stress increases, the cleat width becomes narrower, and the permeability decreases exponentially (Meng et al. 2010, 2011). Meanwhile, many scholars have studied the dynamic changes of permeability under the superposition of multiple factors and established a series of dynamic permeability prediction models based on these factors (e.g., Clarkson et al., 2008; Kumar et al., 2012; Liu et al., 2012; Palmer & Mansoori, 1998; Pan et al., 2010; Shi & Durucan, 2004; Zhou et al., 2020). Moreover, the anisotropy of fractures is expected to affect reservoir characteristics and seepage performance, and further it affects the advantageous seepage channel in coal seam (Zhang et al., 2021). Previous studies found that permeability varies extensively in different directions (relative to bedding plane), and the maximum ratio of permeability in different directions of coal bedding could be 17:1 (Laubach et al., 1998; Li et al., 2004; Wang et al., 2014; Zhang et al., 2021).

Therefore, the effective stress is extremely harmful to coal reservoir permeability, which in turn affects the productivity of CBM wells. However, most of these studies are based on theoretical analysis or laboratory physical simulation, and few researches combine analysis results with production practices. The control effect of SSE on the distribution of high-yield wells has never been reported. Since the commercial development of the Fanzhuang Block (FZ Block) in 2006, more than 1,200 CBM wells have been put into production. However, the gas production rate varies greatly between wells, showing the characteristics of zoning or fragmenta-

**Figure 1** (a) Generalized map showing location of the Qinshui Basin (modified from Lv et al., 2012). (b) Qinshui Basin and CBM commercial development blocks, mainly including Zhengzhuang Block, FZ Block, and Panzhuang Block. (c) Distribution of faults emphasizing the distribution of production wells and sampling location in the FZ Block.

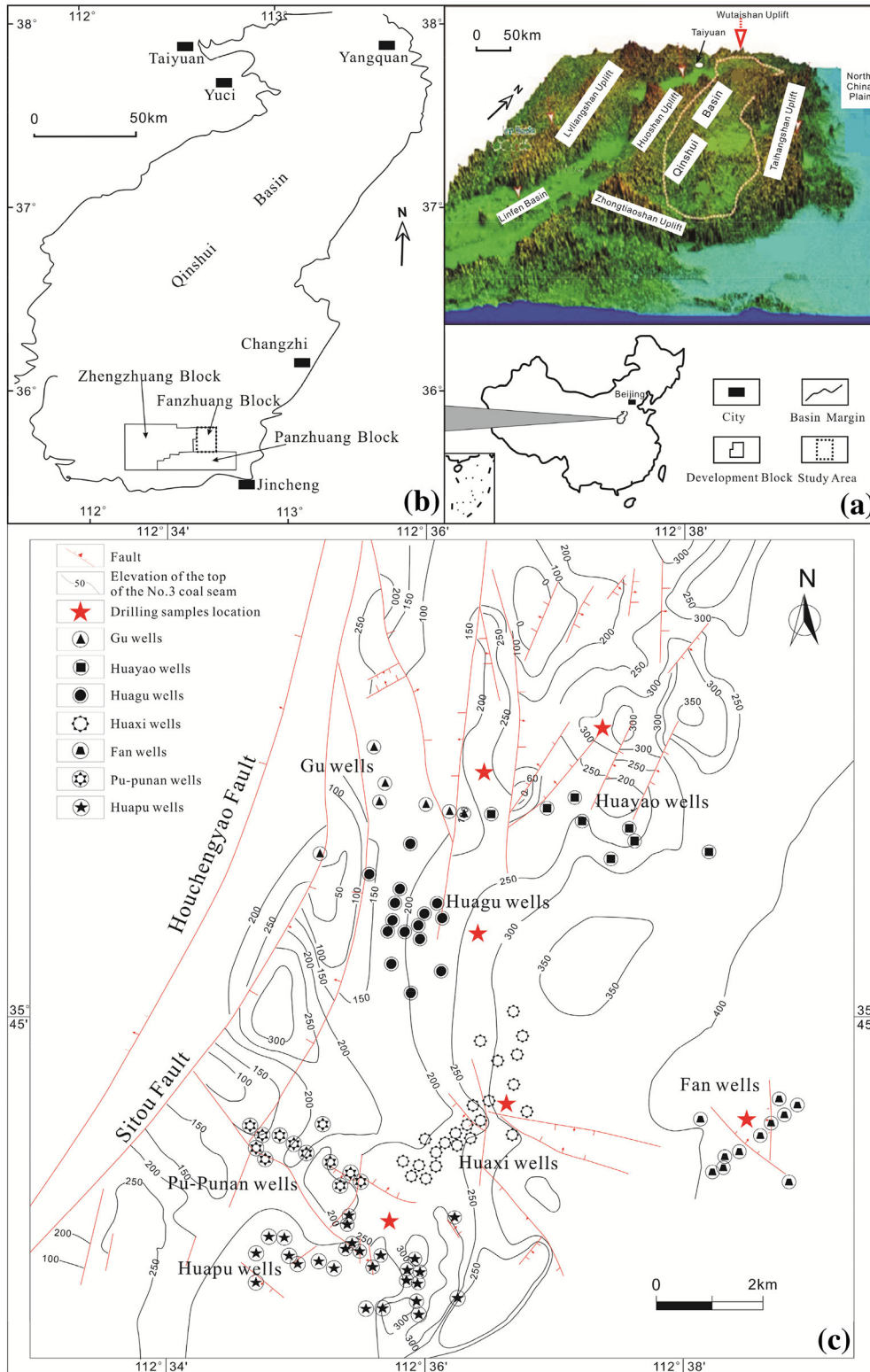
tion changes (Meng et al., 2011; Tao et al. 2014, 2019b). Therefore, understanding the distribution law of high-yield wells and the geological and engineering conditions for forming high-yield wells are of great significance for well deployment and well pattern optimization.

In the current study, based on stress sensitivity experiments and on analysis of gas production from different wells at different drainage stages in the FZ Block, the damage to coal reservoir permeability is caused by the SSE and the corresponding variation of CBM productivity was analyzed. Finally, the distribution of high-yield wells in the FZ Block was discussed, aiming to provide insights for selecting suitable CBM development blocks and making appropriate development strategies.

## GEOLOGICAL SETTING AND SAMPLES

The Qinshui Basin is located in the southeast of Shanxi Province in northern China (Fig. 1a). The long axis of the basin is arranged generally in the NW–SW direction and it is more than 330 km long. The basin is a large synclinorium with symmetrical sides (Lv et al., 2012; Tao et al., 2019c). The main coal-bearing strata are the Carboniferous Taiyuan and the Permian Shanxi Formations. The No. 3 coal seam of the Shanxi Formation is the main target layer for CBM development. The FZ Block is located in the southwest corner of the Qinshui Basin with total gas-bearing area of 398.23 km<sup>2</sup> (Fig. 1b; Su et al., 2005).

Six coal samples were collected from scattered exploration wells in the FZ Block (Fig. 1c), and then coal core samples (about 2.5 cm in diameter and 3–5 cm in length) were prepared using wire cutting method for stress sensitivity experiments (Wan et al., 2015). Meanwhile, another seven cylindrical coal samples (about 5 cm in diameter and 10 cm in length) were drilled from coal blocks for basic physical property testing. These coal blocks were collected from the No. 3 coal seam in the coal mines distributed in the FZ Block.



## SAMPLES AND ANALYTICAL PROCEDURES

Porosity and permeability tests were performed following the method described by Zhao et al. (2015a). Here, permeability was measured based on the unsteady pressure decay method (Jones, 1972). Meanwhile, the measurement was performed at a constant ambient temperature. Porosity and pore volume were calculated by Boyle's law, while permeability was calculated with Darcy's law.

Considering stress gradient of 0.94 MPa/100 m (Ye et al., 1998) and burial depth of the No. 3 coal seam in the FZ Block of 400–1200 m, the confining pressure of the stress sensitivity experiment was set from 3.5 to 15.5 MPa, with a step interval of 2.0 MPa. The specific experimental steps were as follows (Fig. 2):

(1) Load coal sample into core holder, connect the instrument and debug the instrument.

(2) Open helium cylinder to supply gas to the device, and perform leak detection to ensure that device does not leak gas before proceeding with experiment.

(3) Adjust inlet pressure (pump A) to ensure that gas can pass through the entire core. Keep inlet pressure unchanged in subsequent experiments.

(4) A confining pressure of 3.5 MPa was applied to the core holder by the confining pressure pump (pump B) to test the first data point. The confining pressure was maintained for 60 min to ensure that coal deformation reaches equilibrium. Record the corresponding pressure and flow rate after the outlet

flow rate are stable; then, permeability was calculated.

(5) Adjust confining pressure and repeat step (4) to next data point until the experiment is completed.

(6) The confining pressure was gradually reduced from 15.5 to 3.5 MPa, and then the same method was used to measure permeability again for another sample.

Following Zhao et al. (2015b), the maximum permeability damage rate and irreversible damage rate were calculated, respectively, as

$$D_m = \frac{k_0 - k_1}{k_0} \times 100\% \quad (1)$$

$$D_i = \frac{k_0 - k_2}{k_0} \times 100\% \quad (2)$$

where  $D_i$  and  $D_m$  are, respectively, the damage rate (%) and maximum damage rate (%) of coal permeability during the pressure decreasing process,  $k_0$  is the initial permeability (mD<sup>1\*</sup>) of coal core, and  $k_1$  and  $k_2$  are, respectively, the permeability (mD) measured at different pressures during pressure increase and pressure reduction.

The elastic modulus and Poisson's ratio of cylinder coal samples were determined according to GB/T 23,561.7 (2009). In addition, proximate analysis was conducted following the method GB/T 212–2008. Random vitrinite reflectance measurements and maceral analyses (500 points) were performed on polished sections according to ISO 7404.3–1994 (1994) and ISO 7404.5–1994 (1994).

## RESULTS AND DISCUSSION

### Basic Information of Coal Samples

The collected coals had high vitrinite content (71.0–89.1%), followed by inertinite (10.9–29.0%), with vitrinite reflectance ( $R_o$ ) ranging from 2.6 to 3.07%. The result of the proximate analysis shows that the collected samples had relatively low moisture content (0.13–0.4%), low volatile component (6.04–9.68%), and high fixed carbon content (77.76–85.58%) (Table 1). The average elastic modulus and Poisson's ratio of the seven core samples were 4.51 GPa and 0.31, respectively (Table 2).

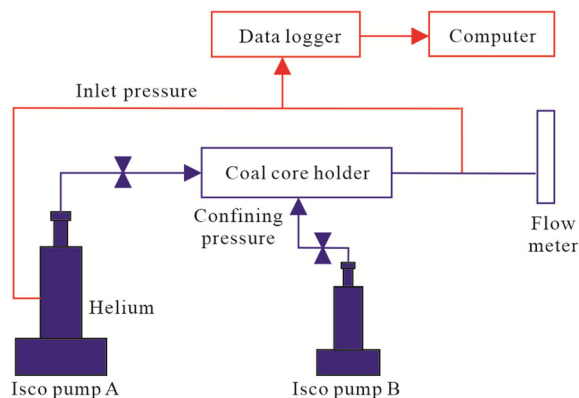


Figure 2. Diagram of coal core stress sensitivity experimental setups.

<sup>1</sup> Millidarcy. 1 mD = 0.9869233 × 10<sup>-3</sup> μm<sup>2</sup>.

**Table 1.** Material composition of the selected coal samples, including results of macerals analysis and proximate analysis

Coal core No	$R_o$ (%)	Relative content of macerals groups (vol%)		Proximate analysis (%)			
		Vitrinite	Inertinite	Moisture	Ash yield	Volatile	Fixed carbon
FS1	2.63	71	29	0.13	6.58	8.58	84.71
FS2	2.95	86.2	13.8	0.29	13.43	6.08	80.2
FS3	3.07	82.3	17.7	0.22	8.16	6.04	85.58
FS4	2.49	74.5	25.5	0.4	12.87	6.74	79.99
FS5	2.19	89.1	10.9	0.16	10.31	7.67	81.86
FS6	2.6	85.9	14.1	0.13	12.43	9.68	77.76

**Table 2.** Elastic modulus, Poisson's ratio, and compressive strength of the selected coal samples

Coal No	cylinder	Diameter (cm)	Height (cm)	Confining pressure (MPa)	Elastic modulus (MPa)	Poisson's ratio	Compressive strength (MPa)
FZ01		5	10.04	5	3572	0.29	33.54
FZ02		5	9.99		5955	0.35	36.24
FZ03		5	10		2846	0.26	30.5
FZ04		4.98	10.13		3624	0.25	35.11
FZ05		5	10		6382	0.36	38.13
FZ06		5	10.04		4917	0.34	36.08
FZ07		5.01	10.03		4276	0.31	34.85
Average		5	10.03		4510	0.31	34.92

**PRODUCTIVITY CHARACTERISTICS IN DIFFERENT PRODUCTION STAGES**

Regional geological setting and coal reservoir properties have great effects on the productivity of CBM wells (e.g., Bachu & Michael, 2003; Palmer, Cameron, et al., 2005; Tao et al., 2019b; Zhao et al., 2015b; Ziarani et al., 2011). The CBM wells in the FZ Block are divided into seven groups including the Gu, Huayao, Huagu, Huaxi, Pu-Punan, Fan, and Huapu Groups. Considering the overall production of CBM wells in the FZ Block as relatively low, wells with gas production rate of 2000 m<sup>3</sup>/day or higher are regarded as high-yield wells. As drainage progresses, the number and distribution of high-yield wells will change.

As shown in Table 3, with the progress of drainage, the gas production rate of wells gradually increases, but the time to reach high production and the number of high-yield wells in different groups is significantly different. Wells with high water production rate in the single-phase water stage always have a longer gas breakthrough time, which means that these wells have experienced a long single-

phase water stage, leading to serious stress sensitivity damage (SSD) to the permeability of coal reservoirs. Moreover, as shown in Fig. 3, after 3 years of production, wells in the Gu, Huagu and Pu-Punan Groups have a NW-SE high-yield distribution trend, while wells in the Huayao and Huaxi Groups have a NE-SW high-yield distribution trend. Due to the low gas content (almost < 15 m<sup>3</sup>) of Huapu and Fan wells, none of the collected 11 wells can achieve high production (Lv et al., 2012). Liu et al. (2008) reported that a very low gas production occurred in high-rank coal reservoir with the gas content lower than 15 m<sup>3</sup>. Thus, the number and distribution of high-yield wells in different groups changed in different drainage stages. On the one hand, it depends on the initial gas content of the coal seam. On the other hand, it is related to the advantageous seepage channel (controlling the expansion direction of the regional pressure drop) in the coal seam formed during the production process, while the latter is closely related to the SSD of reservoir permeability during the CBM development process.



**Table 3.** Average gas and water production rate of high-yield wells in different groups of FZ Block

Group	Well	Average water production (m <sup>3</sup> /day) in single-phase water stage	Average gas production (m <sup>3</sup> /day)					
			0.5 a	1 a	1.5 a	2 a	2.5 a	3 a
Gu	Gu-H1	5.04	2483	3032	2674	2570	2655	2634
	Gu-H2	3.79	261	1396	2411	3005	3921	4725
	Gu-H3	6.63	0	410	1304	1851	2207	2602
	Gu-H4	3.05	390	1648	2364	2814	2888	2891
Huayao	HY-H1	2.03	0	347	889	1257	1676	2063
	HY-H2	1.25	0	1166	1836	2190	2381	2475
	HY-H3	1.78	0	438	1329	2021	2652	2944
	HY-H4	1.54	193	1263	1948	2265	2425	2523
Huagu	HG-H1	4.33	262	1880	2896	3369	3455	3418
	HG-H2	3.43	307	1359	1813	2005	2110	2142
	HG-H3	3.83	409	1892	4059	4643	4806	4914
	HG-H4	12.74	0	253	288	351	1581	2077
	HG-H5	3.60	537	1392	1838	2002	2074	2115
Huaxi	HX-H1	2.86	144	1337	2397	2677	2670	2769
	HX-H2	1.1	1179	1468	1856	2231	2384	2458
	HX-H3	2.27	1282	2875	3312	3398	3431	3384
	HX-H4	1.38	935	2063	2474	2483	2400	2223
	HX-H5	1.3	1488	2324	2367	2290	2191	2182
	HX-H6	2.24	579	1366	1589	1637	1459	2151
	HX-H7	1.89	1308	1762	1724	1633	1544	2017
	HX-H8	2.29	2491	3678	4196	4082	3800	3560
	HX-H9	1.38	2713	3864	4512	4421	4115	3807
	HX-H10	1.73	275	774	1775	2528	2774	2825
Pu-Punan	PuPN-H1	1.94	2225	2092	2348	2527	2640	2592
	PuPN-H2	3.78	249	1471	1404	1404	1851	3640
	PuPN-H3	1.67	971	1183	1412	1626	1775	2006

## CHARACTERIZATION OF ADVANTAGEOUS SEEPAGE CHANNEL THROUGH STRESS SENSITIVITY EXPERIMENT

### Stress Sensitivity Experiment

The initial porosity and permeability of the coal cores were 3.2–5.5% and 0.12–0.54 mD, respectively. All coal cores had strong SSD to coal permeability when the confining pressure reached 15.5 MPa. Among these cores, FS3 had the lowest maximum damage rate of 65.6%, while S4 had the highest of 98.5%. The permeability of coal cores, which have undergone the SSD, cannot be fully recovered even after the stress was released, which indicates that the SSD of the CBM reservoir was irreversible, and the irreversible damage rate varied from 21.9 to 75.9% (Table 4). This may mean irreversible damage to coal permeability due to the inelastic deformation during hydraulic fracturing or CBM development. Therefore, the SSD of reservoir permeability should be limited to a minimum during CBM production.

As shown in Fig. 4, at the initial stage of increasing the confining pressure, the permeability of coal was reduced greatly. The greater the pressure increase, the greater the decrease in permeability. Moreover, the maximum damage rate increased with decrease in permeability. Therefore, on the one hand, the excessively fast drainage rate causes the reservoir pressure to drop too fast, which leads to the reservoir permeability damage caused by effective stress during decompression process (Harpalani & Chen, 1992; Tao et al., 2012; Walsh, 1981). On the other hand, a well with a slow drainage rate will experience a longer single-phase water drainage time, and so the reservoir will suffer continuous SSE, which will make it difficult to restore the permeability of the coal reservoir later. In the development of CBM, the drainage rate should be controlled strictly to maintain a stable pressure drop and reduce the reservoir permeability damage caused by the SSE.

According to Palmer and Mansoori (1996) and Jaeger and Cook (1979), the dynamic change of coal permeability caused by effective stress during the CBM development can be obtained as:

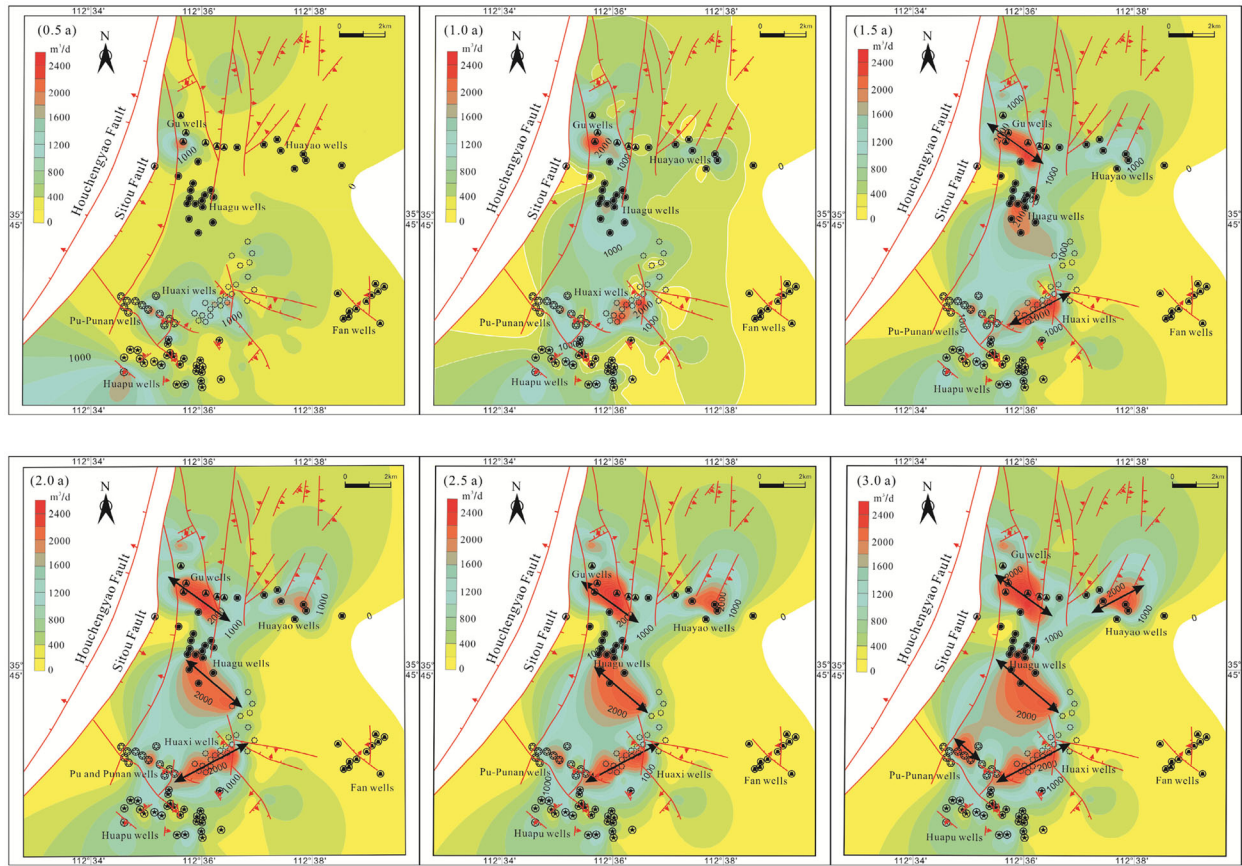


**Figure 3.** Gas production rate of CBM wells in the FZ Block emphasizing the distribution trend of high-yield wells in different production stages. The black double arrow line represents the expansion direction of high-yield areas.

$$k = k_o \left(1 + \frac{p - p_o}{\phi_o M}\right)^3 \quad (3)$$

and the axial modulus is calculated as:

$$M = E \frac{1 - \nu}{(1 + \nu)(1 - 2\nu)} \quad (4)$$

where  $k$  and  $k_o$  are, respectively, the instant permeability (mD) during the CBM development process and the initial permeability,  $p$  and  $p_o$  are, respectively, confining pressure (MPa) and reservoir pressure (MPa),  $\phi_o$  is the initial effective porosity (%),  $M$  and  $E$  are, respectively, axial modulus (MPa) and elastic modulus (MPa), and  $\nu$  is the Poisson's ratio of the axial modulus.

Based on the Eqs. (3) and (4) and the tested mechanical parameters listed in Table 2, the permeability decline caused by effective stress increase during the CBM development can be calculated. A

pressure drop of 3 MPa (i.e.,  $p - p_o = 3$  MPa) will reduce the initial permeability by 4.25% ( $k_o$ ), while pressure drops of 5 MPa and 10 MPa will reduce permeability by 7.01% and 13.7%, respectively. At the same differential pressure point, although the calculated permeability damage values are lower than those measured by the SSE experiment due to the lack of stress release process, the damage to the coal reservoir in the FZ block with extremely low initial permeability is still serious (Meng et al., 2011).

### Cleat Compressibility Controls Advantageous Seepage Channel

Considering the dynamic change of permeability, the sensitivity of permeability to effective stress increase can be expressed as:

**Table 4.** Maximum and irreversible damage rate of coal cores

Coal cores	Porosity (%)	$R_o$ (%)	Length (cm)	Diameter (cm)	Permeability (mD)	Maximum damage rate (%)	Irreversible damage rate (%)
FS1	5.5	2.63	2.726	2.568	0.54	94.4	75.9
FS2	5.5	2.95	2.975	2.560	0.13	90.5	63.5
FS3	4.1	3.07	4.610	2.550	0.10	65.6	21.9
FS4	4.1	2.49	3.144	2.540	0.12	98.5	40.0
FS5	5.4	2.19	3.713	2.563	0.22	85.4	49.8
FS6	3.2	2.6	3.424	2.562	0.14	93.9	41.8

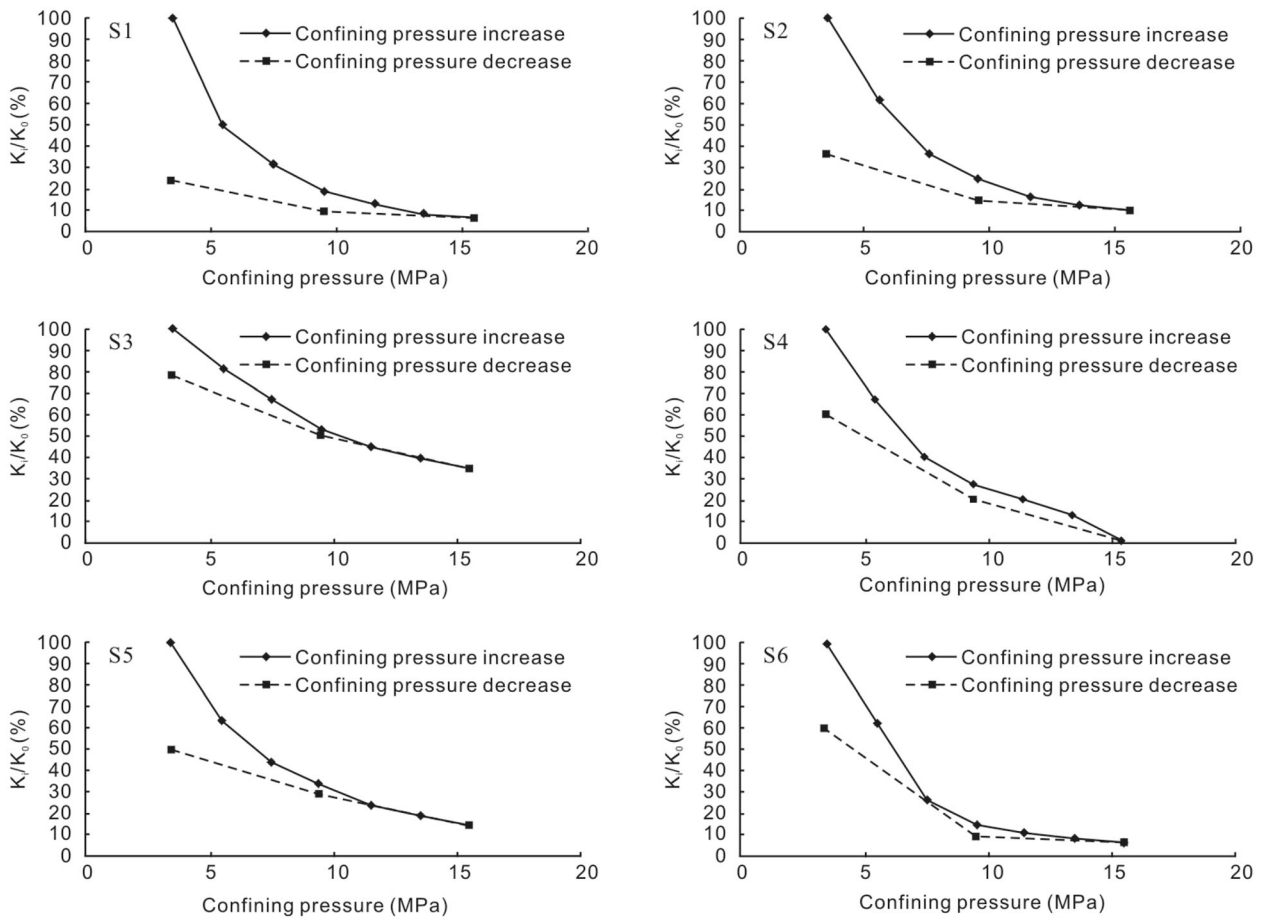


**Figure 4.** Change of coal core permeability with adding and unloading confining pressure.

$$k = k_0 e^{-3C_f \Delta\sigma} \tag{5}$$

where  $C_f$  is cleat compressibility ( $\text{MPa}^{-1}$ ), and  $\Delta\sigma$  is the effective stress (MPa) difference. If the two sides

of the Eq. (5) are taken as logarithms, it can be rewritten as:

$$-\frac{1}{3} \ln \frac{k}{k_0} = C_f \Delta\sigma \tag{6}$$



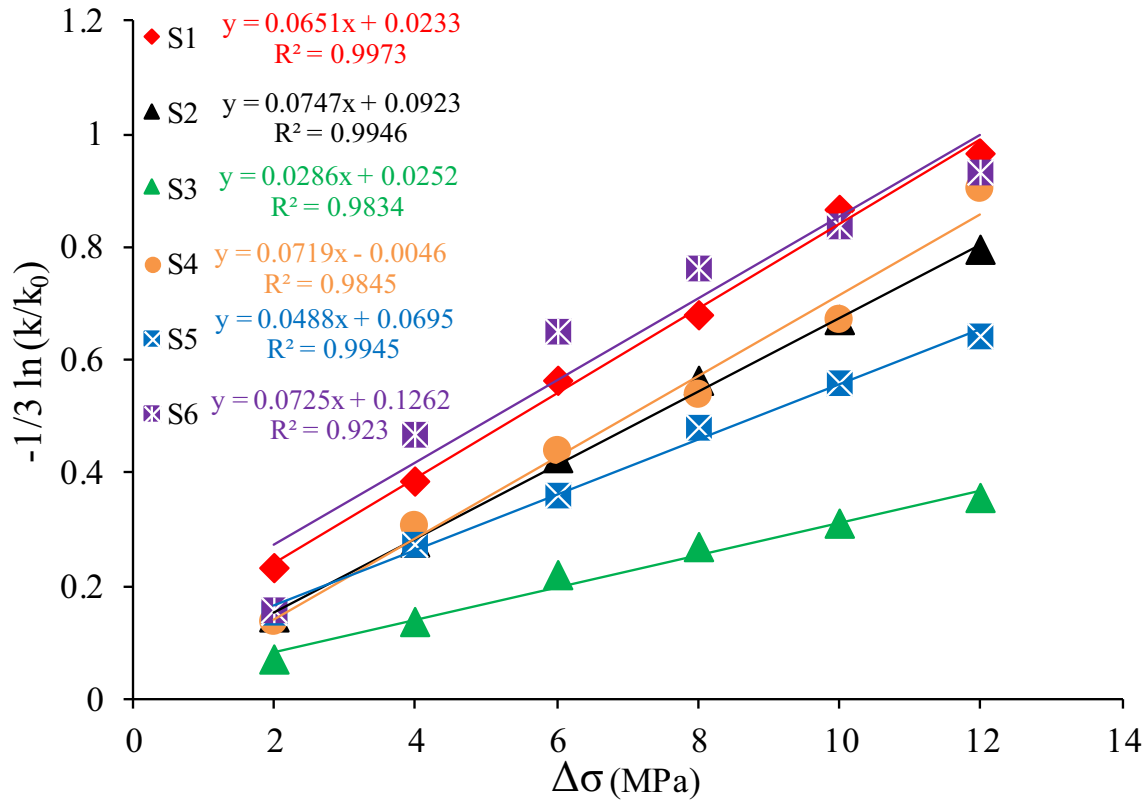


Figure 5. Fitting of effective stress difference versus permeability ratio identifying cleat compressibility.

Equation (6) indicates that the change rate of permeability and the variation of effective stress have a linear relationship in the semi-logarithmic coordinate system. Cleat compressibility can be determined quantitatively as the slope of the fitted curve between  $-1/3 \ln(k/k_0)$  and  $\Delta\sigma$ . Cleat compressibility is written as:

$$C_f = \frac{-\frac{1}{3} \ln \frac{k}{k_0}}{\Delta\sigma} \tag{7}$$

Therefore, in the semi-logarithmic coordinate system, the horizontal axis is the effective stress difference ( $\sigma - \sigma_0$ ), the vertical axis is the  $(-1/3 \ln(k/k_0))$ , and the slope of the fitting curve is the cleat compressibility under the condition of the stress difference ( $\sigma - \sigma_0$ ), which is a significant coefficient reflecting permeability loss as the effective stress increases. Figure 5 indicates that the permeability ratio of the six coal samples increased with the effective stress as the confining pressure

increased from 3.5 to 15.5 MPa. Here, the cleat compressibility varied between 0.0286 and 0.0725 MPa<sup>-1</sup> (average 0.06 MPa<sup>-1</sup>), but the variation range was relatively small, which indicates that pore-fracture system of high-rank coal was poorly developed, and the compressibility was weak, resulting in the similar cleat compressibility of these samples.

Figure 6 shows that as the effective stress difference increased, the cleat compressibility of the sample increased or decreased, but overall showing a decreasing trend. It also suggests that the dynamic variation of permeability was essentially the compression and deformation of coal reservoir cleats under the action of effective stress, and the increase in pore-fracture compression had a good consistency with increase in pressure difference.

Therefore, it can be found that cleat compressibility is not a fixed value under different effective stress difference. Shi and Durucan (2004)

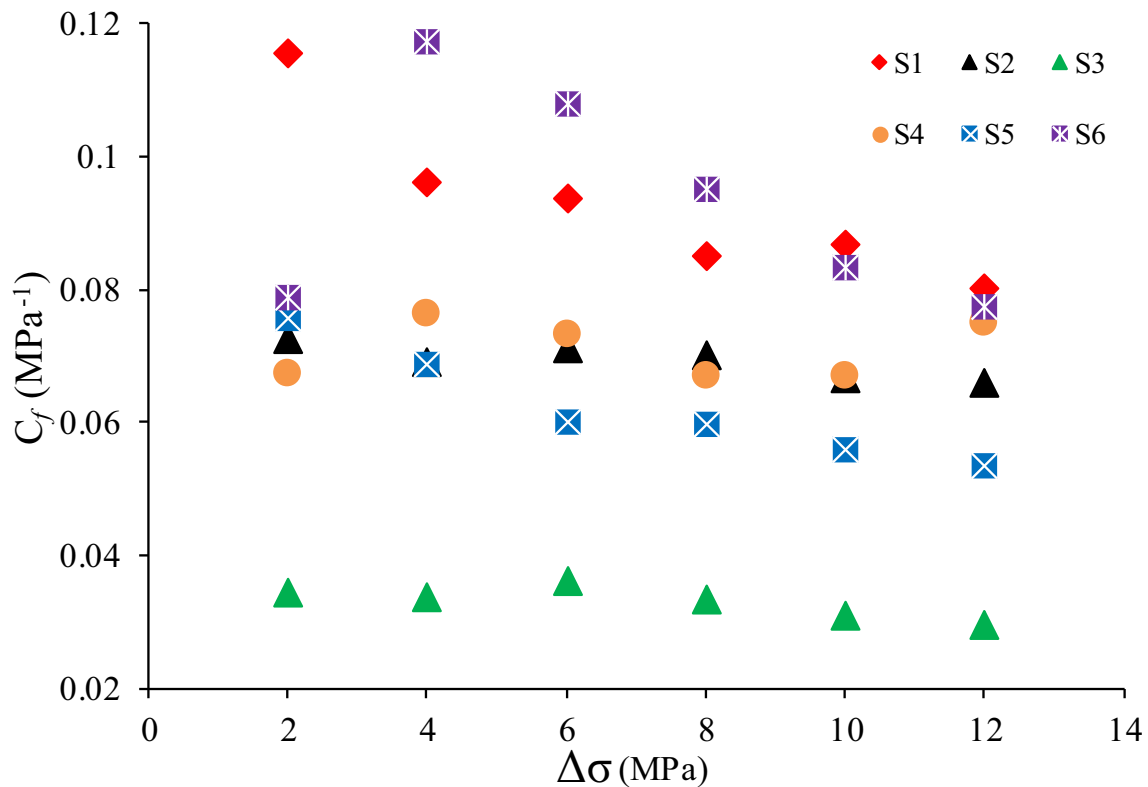


Figure 6. Dynamic variation of cleat compressibility under different effective stress difference.

noted that under biaxial stress, both permeability and horizontal stress strongly influence the determination of cleat compressibility. Zheng et al. (2012) suggested that as pore pressure increases, cleat compressibility first decreases and then increases slightly. Gensterblum et al. (2014) indicated that due to the orientation of the cleat, its compressibility might be affected by the variation of multi-slip flow. During the development of CBM, due to the influence of effective stress, the coal reservoir cleat undergoes compression deformation, and permeability changes dynamically, which in turn controls CBM production. For high-rank coal reservoirs, although the compression of the cleat is limited by a single factor, the superposition of multiple factors will inevitably lead to an increase in cleat compression in a certain direction, while the cleat compression in the opposite direction is relatively smaller. In this case, an advantageous seepage channel is formed, which in turn controls the expansion direction of high-yield wells.

#### INFLUENCE OF ADVANTAGEOUS SEEPAGE CHANNEL ON THE DISTRIBUTION OF HIGH-YIELD WELLS

The development of CBM is a process of drainage and pressure reduction, which inevitably causes SSE in coal reservoirs. The gas production rate is influenced by different levels of cleat compression under different reservoir conditions, working systems, and development stages. According to the variation characteristics of gas production rate at different development stages in the FZ Block, combined with regional geological conditions, the influence of SSE on CBM production at different development stages is discussed below.

#### Tectonic Stress Field

According to fracturing monitoring reports, the predominant extension direction of fracturing frac-

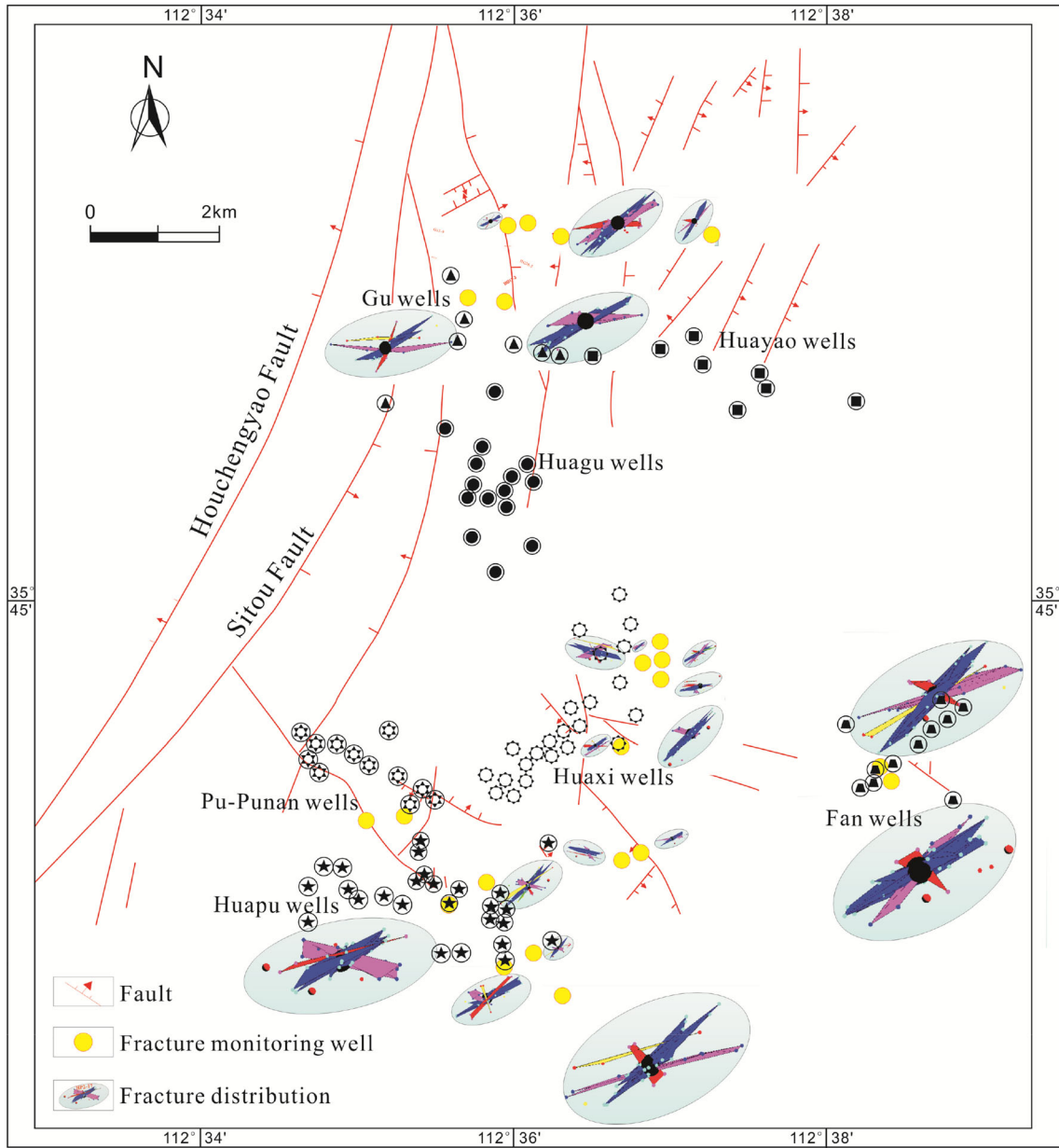


Figure 7. Fracturing fracture distribution of No. 3 coal seam in the FZ Block.

tures in the FZ Block is NNE (Fig. 7), which reflects that the present in situ stress orientation is ENE–WSW. Meng et al. (2010) obtained the same results based on 45 hydraulic fracturing test data. They proposed that the principal compressional axis orientation of the tectonic stress field is ENE, with an elevation angle of 10°, and the principal tensile axis orientation is NNW, with elevation angle varies between 30° and 50°. Therefore, the tectonic stress

field in the study area is characterized by near-horizontal extrusion in the ENE–WSW direction and tensile stress in the NNW–SSE direction.

By analyzing the productivity variation of CBM wells at different stages and the distribution of the wells, it can be considered that the Gu and Huagu wells with high gas production rate extend from NW to SE, while for the Huayao group, the distribution of high-yield wells shows the direction from NE to

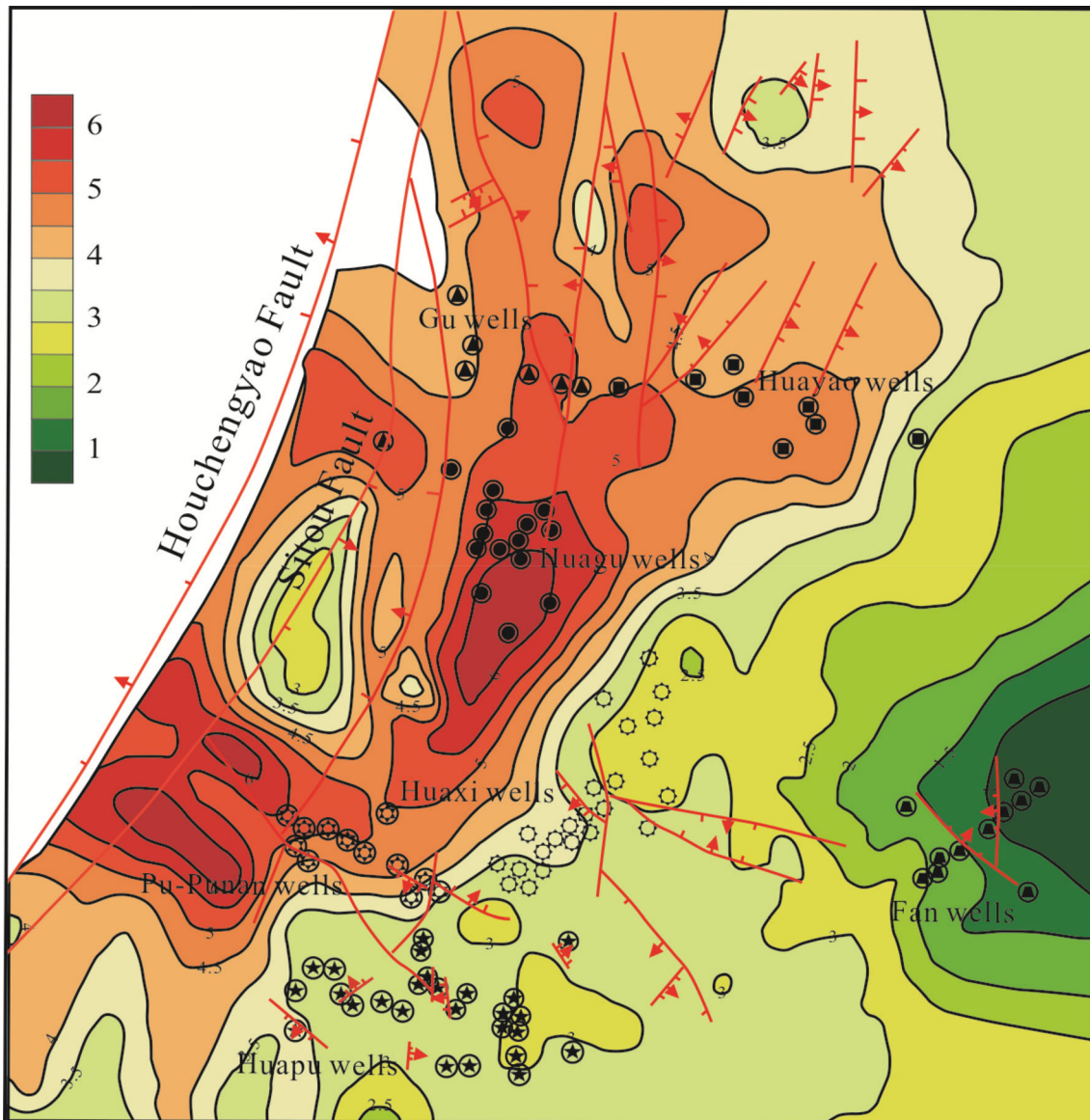


Figure 8. Reservoir pressure distribution of No. 3 coal seam in the FZ Block.

SW. As shown in Table 3, the water production rate of Gu wells (averaging  $4.63 \text{ m}^3/\text{day}$ ) and Huagu wells (averaging  $5.59 \text{ m}^3/\text{day}$ ) in the early production stage is higher than that of Huayao wells (averaging  $1.65 \text{ m}^3/\text{day}$ ) and Huaxi wells (averaging  $1.84 \text{ m}^3/\text{day}$ ). Generally, a large amount of produced water means a large pressure drop range (Lv et al., 2012; Tao et al., 2012). Therefore, the Gu and Huagu CBM wells appeared to have suffered strong SSE according to the experimental simulation results. Moreover, according to the distribution of tectonic

stress field, the SSD to coal reservoir is relatively weak in NNW–SSE orientation due to the tensile stress condition so that the pressure drop funnel can be effectively extended, and a large desorption area can be achieved in this direction. The SSD is much greater along the ENE–WSW orientation under the near-horizontal extrusion condition, which leads to a decrease in reservoir permeability. The depressurization is difficult and the pressure drop is limited in this direction. Therefore, the desorption and migration capacity of CBM are much weaker in

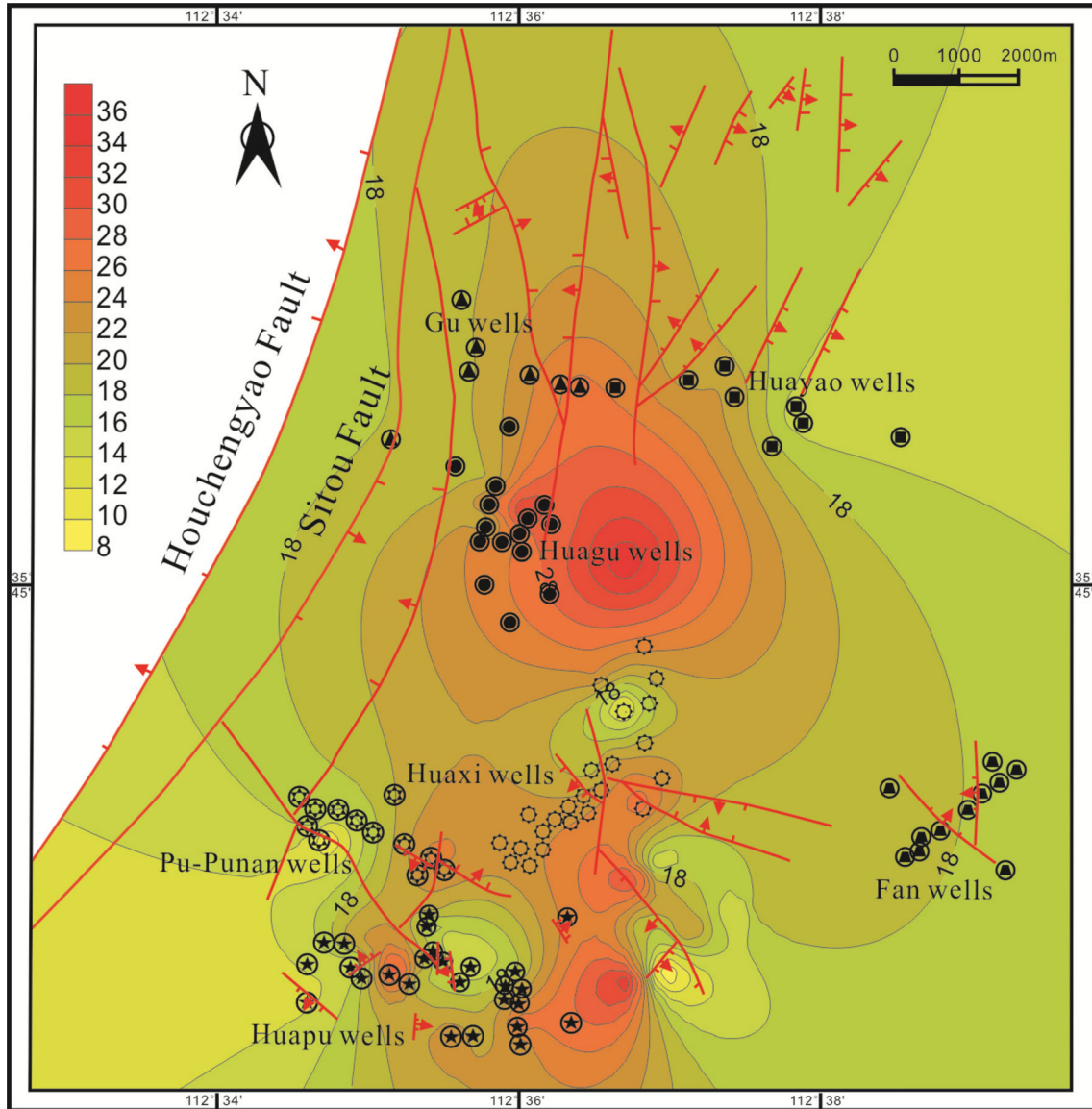


Figure 9. Fracture pressure distribution of No. 3 coal seam in the FZ Block.

wells in the ENE–WSW direction than those in wells in the NNW–SSE direction. The water production rate of Huayao wells in the early production stage is relatively low and the SSD to reservoirs is small. At the same time, the direction of predominant fracturing fractures is ENE–WSW, so the dominant direction of high-yield wells of Huayao group is consistent with the direction of the predominant fractures.

### Reservoir Pressure

As shown in Fig. 8, the coal reservoir pressure varies greatly in the FZ Block. The reservoir pressure in the Gu, Pu-Punan and Huagu wells is greater than 4.5 MPa, and the reservoir pressure in the Huapu, Huayao and Huaxi wells is between 3 and 4.5 MPa, while the Fan wells have relatively low reservoir pressure, lower than 3 MPa. High reservoir pressure usually corresponds to high gas content in coal (Tang et al., 2016; Zhu et al., 2017), and so high-yield wells are usually distributed in areas with high



reservoir pressure. Figure 8 shows that most high-yield wells are located in areas where the reservoir pressure is greater than 4 MPa. However, in the FZ Block, many coal reservoirs have low gas saturation, and average ratio of critical desorption pressure to reservoir pressure is only 0.5 on average (Lv et al., 2012). In the drainage stage, areas with high reservoir pressures usually require rapid drainage and pressure reduction to reach the critical desorption pressure. Thus, high reservoir pressure areas often go through a long period of single-phase water drainage, and coal reservoirs have stronger SSD, which in turn controls the distribution of high-yield wells.

The Gu, Huagu, and Pu-Punan wells have relatively high reservoir pressure, which causes a large pressure drop and a long single-phase water drainage time, leading to strong SSE on coal reservoir in the predominant fracture direction and the expansion of pressure drop funnel is restricted. Therefore, the distribution of high-yield wells in the Gu, Pu-Punan, and Huagu areas is in the NW–SE direction (tensile stress direction), which is perpendicular to the direction of predominant fractures. In contrast, the reservoir pressures of Huayao and Huaxi wells are relatively low, and so the critical desorption pressure can be reached with a small pressure drop. Therefore, the SSE on the shape of predominant fractures is weak, which is conducive to form a regional pressure drop funnel along the direction of predominant fractures, and it is the distribution direction of high-yield wells. Therefore, in the initial stage of drainage, the pressure drop rate should be reasonably controlled in the high reservoir pressure area to avoid severe reservoir damage caused by SSE.

### Fracture Pressure of Coal Reservoir

Fracture pressure is determined mainly by the in situ stress properties and tensile strength. Under condition of a certain in situ stress, the smaller the tensile strength, the lower the fracture pressure (Zhu et al., 2009). Based on the fracturing reports of the FZ Block, the fracture pressure of No.3 coal seam is presented in Fig. 9. Comparing the distribution of high-yield wells (Fig. 3), it can be seen that high-yield wells are always located in areas with high fracture pressure (Fig. 9). This is because the coal reservoir with high fracture pressure has a relatively high tensile strength and the SSD of coal reservoir is

relatively weak, which is conducive to the expansion of the pressure drop funnel and increases the desorption area of the CBM well.

### CONCLUSIONS

(1) All the coal cores samples have strong SSD with increasing in confining pressure. Among the test samples, FS3 had the lowest maximum permeability damage rate of 65.6%, and FS4 had the highest of 98.5%. The coal permeability could not be fully recovered after the stress was unloaded, indicating that the SSD in the CBM reservoirs was irreversible, and the irreversible damage rate varied greatly, from 21.9% to 75.9%. The cleat compressibility varied between 0.0286 and 0.0725 MPa<sup>-1</sup>.

(2) The gas production rate of CBM wells changes dramatically in the FZ Block, and only a few of them can reach high-yield. During the development process of CBM, under the action of effective stress, an advantageous seepage channel will be formed in the coal seam, which determines the expansion direction of high-yield wells. The Gu, Huagu, and Pu-Punan Groups have high-yield wells with NW–SE distribution, while the Huayao and Huaxi Groups have high-yield wells with NE–SW distribution.

(3) The development of CBM is a process of drainage and pressure reduction, which causes inevitable stress-related damage to coal reservoirs. Therefore, during the development process of CBM, effective measures should be taken to reduce permeability damage of coal reservoirs caused by effective stress, such as controlling the rate of drainage. At the same time, factors such as tectonic stress field, coal reservoir pressure and coal fracture pressure should also be considered to find advantageous seepage channels and deploy wells along these channels to increase the production rate of CBM wells.

### ACKNOWLEDGMENTS

This work was financially supported by the National Natural Science Foundation of China (41772132, 41502157, 41530314), the Key Project of the National Science & Technology (2016ZX05044-001), and the Fundamental Research Funds for the Central Universities (2652019095).

## REFERENCES

- Bachu, S., & Michael, K. (2003). Possible controls of hydrogeological and stress regimes on the producibility of coalbed methane in upper Cretaceous–tertiary strata of the Alberta basin, Canada. *AAPG Bulletin*, 87, 1729–1754.
- Bell, J. S. (2006). In-situ stress and coal bed methane potential in Western Canada. *Bulletin of Canadian Petroleum Geology*, 54, 197–220.
- Chen, S. D., Tang, D. Z., Tao, S., Xu, H., Li, S., Zhao, J. L., et al. (2018). Characteristics of in-situ stress distribution and its significance on the coalbed methane (CBM) development in Fanzhuang-Zhengzhuang Block, Southern Qinshui Basin, China. *Journal of Petroleum Science and Engineering*, 161, 108–120.
- Clarkson, C. R., Pan, Z., Palmer, I., & Harpalani, S. (2008). Predicting sorption-induced strain and permeability increase with depletion for CBM reservoirs. *SPE Journal*, 14, 152–169.
- GB/T 23561.7, (2009). Chinese national standard. Coal and rock, Method of determining physical and mechanical properties (in Chinese).
- Harpalani, S., & Chen, G. (1992). Effect of gas production on porosity and permeability of coal. In: Beamish, BB, Gamson, PD (Eds.), Symposium on Coalbed Methane, Townsville, Australia 4, 67.
- ISO 7404.3–1994, (1994). Methods for the petrographic analysis of bituminous coal and anthracite-part 3: Method of determining maceral group composition.
- ISO 7404.5–1994, (1994). Method for the petrographic analysis of bituminous coal and anthracite-part 5: Method of determining microscopically the reflectance of vitrinite. MOD.
- Jaeger, J. C., & Cook, N. G. W. (1979). *Fundamentals of rock mechanics* (3rd ed.). Chapman and Hall Press.
- Jones, S. C. (1972). A rapid accurate unsteady-state klinkenberg permeameter. *SPE Formation Evaluation*, 12, 383–397.
- Kumar, H., Elsworth, D., Liu, J., Pone, D., & Mathews, J. P. (2012). Optimizing enhanced coalbed methane recovery for unhindered production and CO<sub>2</sub> injectivity. *International Journal of Greenhouse Gas Control*, 11, 86–97.
- Laubach, S. E., Marrett, R., Olson, J., & Scott, A. R. (1998). Characteristics and origins of coal cleat: A review. *International Journal of Coal Geology*, 35, 174–207.
- Li, H. Y., Shimada, S., & Zhang, M. (2004). Anisotropy of gas permeability associated with cleat pattern in a coal seam of the Kushihiro coalfield in Japan. *Environmental Geology*, 47(1), 45–50.
- Li, Y., Tang, D. Z., Xu, H., Meng, Y. J., & Li, J. Q. (2014). Experimental research on coal permeability: The roles of effective stress and gas slippage. *Journal of Natural Gas Science and Engineering*, 21, 481–488.
- Liu, R. H., Liu, F., Zhou, W., Li, J. M., & Wang, H. Y. (2008). An analysis of factors affecting single well deliverability of coalbed methane in the Qinshui Basin. *Natural Gas Industry*, 28(7), 30–33. (in Chinese with English abstract).
- Liu, S., Harpalani, S., & Pillalamarry, M. (2012). Laboratory measurement and modeling of coal permeability with continued methane production: Part 2-Modeling results. *Fuel*, 94, 117–124.
- Lv, Y. M., Tang, D. Z., Xu, H., & Luo, H. H. (2012). Production characteristics and the key factors in high-rank coalbed methane fields: A case study on the Fanzhuang Block, Southern Qinshui Basin, China. *International Journal of Coal Geology*, 96–97, 93–108.
- Mazumder, S., Scott, M., & Jiang, J. (2012). Permeability increase in Bowen basin coal as a result of matrix shrinkage during primary depletion. *International Journal of Coal Geology*, 96–97, 109–119.
- Men, X. Y., Tao, S., Liu, Z. X., Tian, W. G., & Chen, S. D. (2021). Experimental study on gas mass transfer process in a heterogeneous coal reservoir. *Fuel Processing Technology*, 216, 106779.
- Meng, Z. P., Tian, Y. D., & Li, G. F. (2010). Characteristics of in-situ stress field in Southern Qinshui Basin and its research significance. *Journal of China Coal Society*, 35(6), 975–981. (in Chinese with English abstract).
- Meng, Z. P., Zhang, J. C., & Wang, R. (2011). In-situ stress, pore pressure and stress-dependent permeability in the Southern Qinshui Basin. *International Journal of Rock Mechanics and Mining Sciences & Geomechanics Abstracts*, 48, 122–131.
- Palmer, I. D., Cameron, J. R., & Moschovidis, Z. A. (2005). Looking for permeability loss or gain during coalbed methane production. Paper 0515, 2005 Int. Coalbed Methane Symp., Tuscaloosa, AL, May 17–19. 19p.
- Palmer, I., & Mansoori, J. (1996). How permeability depends on stress and pore pressure in Coalbed: a new model. SPE. 557–563.
- Palmer, I., & Mansoori, J. (1998). How permeability depends on stress and pore pressure in coalbeds: A new model. *SPE Reservoir Evaluation and Engineering*, 1, 539–544.
- Pan, Z. J., Connell, L. D., & Camilleri, M. (2010). Laboratory characterisation of coal reservoir permeability for primary and enhanced coalbed methane recovery. *International Journal of Coal Geology*, 82(3–4), 252–261.
- Seidle, J., & Huitl, L. (1995). *Experimental measurement of coal matrix shrinkage due to gas desorption and implications for cleat permeability increases*. Society of Petroleum Engineers.
- Shi, J. Q., & Durucan, S. (2004). Drawdown induced changes in permeability of coalbeds: A new interpretation of the reservoir response to primary recovery. *Transport in Porous Media*, 56, 1–16.
- Su, X., Lin, X., Liu, S., Zhao, M., & Song, Y. (2005). Geology of coalbed methane reservoirs in the Southeast Qinshui Basin of China. *International Journal of Coal Geology*, 62, 197–210.
- Tang, D. Z., Zhao, J. L., Xu, H., Li, Z. P., Tao, S., & Li, S. (2016). Material and energy dynamic balance mechanism in middle-high rank coalbed methane (CBM) systems. *Journal of China Coal Society*, 41(1), 40–48. (in Chinese with English abstract).
- Tao, S., Chen, S. D., & Pan, Z. J. (2019). Current status, challenges, and policy suggestions for coalbed methane industry development in China: A review. *Energy Science & Engineering*, 00, 1–16.
- Tao, S., Pan, Z. J., Chen, S. D., & Tang, S. L. (2019). Coal seam porosity and fracture heterogeneity of marcolithotypes in the Fanzhuang Block, southern Qinshui Basin, China. *Journal of Natural Gas Science and Engineering*, 66, 148–158.
- Tao, S., Pan, Z. J., Tang, S. L., & Chen, S. D. (2019). Current status and geological conditions for the applicability of CBM drilling technologies in China: A review. *International Journal of Coal Geology*, 202, 95–108.
- Tao, S., Tang, D. Z., Xu, H., Gao, L. J., & Fang, Y. (2014). Factors controlling high-yield coalbed methane vertical wells in the Fanzhuang Block, Southern Qinshui Basin. *International Journal of Coal Geology*, 134–135, 38–45.
- Tao, S., Wang, Y. B., Tang, D. Z., Xu, H., Lv, Y. M., He, W., et al. (2012). Dynamic variation effects of coal permeability during the coalbed methane development process in the Qinshui Basin, China. *International Journal of Coal Geology*, 93, 16–22.
- Walsh, J. B. (1981). Effect of pore pressure and confining pressure on fracture permeability. *International Journal of Rock Mechanics & Mining Sciences & Geomechanics Abstracts*, 18, 429–435.
- Wan, Y., Pan, Z., Tang, S., Connell, L. D., Down, D. D., & Camilleri, M. (2015). An experimental investigation of dif-

- fusivity and porosity anisotropy of a Chinese gas shale. *Journal of Natural Gas Science and Engineering*, 23, 70–79.
- Wang, K., Zang, J., Wang, G. D., & Zhou, A. T. (2014). Anisotropic permeability evolution of coal with effective stress variation and gas sorption: Model development and analysis. *International Journal of Coal Geology*, 130(15), 53–65.
- Yan, Z. M., Wang, K., Zang, J., Wang, C., & Liu, A. (2019). Anisotropic coal permeability and its stress sensitivity. *International Journal of Mining Science and Technology*, 29(3), 507–511.
- Ye, J. P., Qin, Y., & Lin, D. Y. (1998). *Chinese coalbed methane resources*. Xuzhou (in Chinese): China University of Mining and Technology Press.
- Zhang, J., Wei, C., Ju, W., Yan, G., Lu, G., Hou, X., et al. (2019). Stress sensitivity characterization and heterogeneous variation of the pore-fracture system in middle-high rank coals reservoir based on nmr experiments. *Fuel*, 238, 331–344.
- Zhang, T.Y., Tao, S., Tang, D.Z., Tang, S.L., Xu, H., Zhang, A.B., Pu, Y.F., Liu, Y.Y., & Yang, Q. (2021). Permeability anisotropy in high dip angle coal seam: A case study of southern Junggar Basin. *Natural Resources Research*. <https://doi.org/10.1007/s11053-021-09831-7>.
- Zhao, J. L., Tang, D. Z., Lin, W. J., Xu, H., Li, Y., Tao, S., et al. (2015). Permeability dynamic variation under the action of stress in the medium and high rank coal reservoir. *Journal of Natural Gas Science and Engineering*, 26, 1030–1040.
- Zhao, J. L., Tang, D. Z., Xu, H., Lv, Y. M., & Tao, S. (2015). High production indexes and the key factors in coalbed methane production: A case in the Hancheng block, southeastern Ordos basin, China. *Journal of Petroleum Science and Engineering*, 130, 55–67.
- Zheng, G. Q., Pan, Z. J., Chen, Z. G., Tang, S. H., Connell, L. D., Zhang, S. H., et al. (2012). Laboratory study of gas permeability and cleat compressibility for CBM/ECBM in Chinese coals. *Energy Exploration & Exploitation*, 30, 451–476.
- Zhou, H. W., Zhang, L., Wang, X. Y., Rong, T. L., & Wang, L. J. (2020). Effects of matrix-fracture interaction and creep deformation on permeability evolution of deep coal. *International Journal of Rock Mechanics and Mining Sciences*, 127, 104236.
- Zhu, B. C., Tang, S. H., Yan, Z. F., & Zhang, J. Z. (2009). Effects of crustal stresses and natural fractures of fracture pressure of coal reservoirs. *Journal of China Coal Society*, 34(9), 1199–1202. (in Chinese with English abstract).
- Zhu, Q. Z., Tang, D. Z., Zuo, Y. Q., Tao, S., Zhang, L. W., & Geng, Y. G. (2017). Permeability dynamic variation features of coal reservoir in exploitation process of Fanzhuang Block. *Coal Science and Technology*, 45(7), 85–92. (in Chinese with English abstract).
- Ziarani, A. S., Aguilera, R., & Clarkson, C. R. (2011). Investigating the effect of sorption time on coalbed methane recovery through numerical simulation. *Fuel*, 90, 2428–2444.